Light-induced generation of radicals on semiconductor-free carbon photocatalysts

Light-induced generation of radicals on semiconductor-free carbon photocatalysts

Leticia F. Velasco[1], Valter Maurino[2], Enzo Laurenti[2], Conchi Ania[1]*

[1] Instituto Nacional del Carbón, INCAR-CSIC, Apdo. 73, 33080 Oviedo, Spain

[2] Dip. di Chimica, Università di Torino, Via P. Giuria 5-7, 10125 Torino, Italy.

*Corresponding author. Tel.: +34 985 118846; Fax: +34 985 297662. E-mail address: conchi.ania@incar.csic.es (CO Ania)

Keywords: hydroxyl radicals, semiconductor-free carbon photocatalysts, electron spin resonance

Abstract

This work provides an experimental evidence of the photoinduced generation of radical species upon UV irradiation of aqueous suspensions of carbon materials with varied textural, structural and chemical composition. The use of a powerful spectroscopic tool as spin trapping electron spin resonance (ESR) has allowed to detect and identify these radicals (among which are hydroxyl, superoxide and other organic radicals), which are the basis of the so-called Advanced Oxidation Processes. Our results demonstrate the ability of carbon materials -including activated carbons- to interact with UV light, and also to generate highly reactive species capable of promoting the photooxidation of an aromatic pollutant. Moreover, for some of the carbons the concentration of radicals was higher than that detected for titania powders. Although the photogeneration of radicals upon irradiation is a well-known process for inorganic semiconductors such as titanium oxide or zinc oxide, our results demonstrate a similar behavior on carbon materials in the absence of semiconductor additives.

.

1. Introduction

The use of light energy is particularly useful in environmental chemistry, since the excitation of electronic molecular states at energies provided by light (typically UV) may induce chemical bond breaking/synthesis in mild conditions [1]. For this reason, heterogeneous photocatalysis based on semiconductors has become a promising green chemistry technology. Major cornerstones that prevent the large scale implementation of photocatalytic processes are related to the low photonic yields associated to present semiconductors. Crucial points are the correct engineering of optical and photoelectrochemical properties of semiconductors, for which the control over photocatalysts nanostructure has recently received increasing attention [2]. Among different approaches, the coupling of carbon materials as additives to semiconductors has emerged as an effective strategy to improve the photodegradation yields of the resulting carbon/semiconductor composites [3].

In earlier investigations, we have reported the singular photochemical response of activated carbon when exposed to UV light in the absence of semiconductor additives [4, 5] showing their ability to promote the photooxidation of phenol from solution beyond the so-called synergistic effect due to confinement effects and direct photolysis. The origin of this photochemical behavior of activated carbons has been rather controversial since it does not seem to be an intrinsic property of all carbons [5,6] but rather dependent on the characteristics (composition and structure) of the carbon material itself.

However, although direct interactions occurring between UV light and activated carbons have been unambiguously demonstrated [5], still the exact nature and implications of the likely photo-induced process occurring at the carbon upon illumination remains rather unclear. Another issue of concern seems to be if this effect arises from the carbon matrix itself

disregarding any contribution of inorganic species (i.e., ash content) that are commonly present in carbons and that could eventually be photoactive.

Bearing all this in mind, we herein report the first experimental evidence provided by spin trapping electron spin resonance (ESR) spectroscopy that demonstrates the photogeneration of radical species when semiconductor-free carbons are exposed to UV illumination in an aqueous medium. A series of carbon materials with varied structural, textural and chemical composition have been investigated. The formation of paramagnetic species in solution during irradiation of the carbon suspensions was detected by a nitrone spin trapping agent that allow the detection of short-lived free radicals present in aqueous solution at very low concentrations [7,8], otherwise non detectable by conventional ESR spectroscopy.

2. Experimental

2.1 Materials

A series of carbon materials with different textural and chemical characteristics were selected for this study, covering micro- and mesoporous activated carbons (AC1, AC2, AC3, AC4, AC5, AC6), carbons obtained from hydrothermal carbonization of polysaccharides (CS, CSH800), and graphitized carbons (GR1). All the carbons were extensively washed in water and dried at 60 ºC overnight before their use. In the case of AC3, an acid digestion treatment (HF/HCl) was carried out following the method proposed by Korver [9], so as to remove the inorganic impurities (mineral matter). Briefly, about 10 g of the pristine carbon were introduced in a PTFE vessel and sequentially immersed in 100 mL of the following acids: HCl 5M, HF 40% and HCl 35%; the suspension was covered with a PTFE plate and heated at 55-60 ºC (2º C/min) under continuous agitation for 6 hours, and finally rinsed in water until constant pH. The de-ashed carbon was labeled as AC6.

The main physicochemical and textural properties of the selected carbons are compiled in Tables 1 and 2. For comparison, commercially available titania powders (P25, Evonik) were also investigated as a reference material.

2.2 Photodegradation tests

The photoactivity under UV light of all the carbon materials was evaluated towards phenol degradation in water. Experimental details have been reported elsewhere [4,5]. Briefly, about 1 g/L of the carbon was placed in the reactor containing 400 mL of phenol solution (in distilled non buffered water) of initial concentration 100 mg L^{-1}. kinetics studies from batch experiments at room temperature. The UV irradiation source was provided by a high pressure mercury lamp (Helios Italquartz, 125 W, emitting at 313, 360, 404, 436, 546, 577 and 579 nm) vertically suspended in a cylindrical, double-walled quartz jacket cooled by flowing water, immersed in the solution. The suspensions were vigorously stirred (600 rpm) and small aliquots of the solution (~1.5 mL) were taken out at regular time intervals and analyzed by reverse-phase HPLC (Spherisorb C18 column 125 mm· 4mm), using methanol–water mixture (5:95) as mobile phase, using a photodiode array detector. The samples were previously filtered using regenerated cellulose filter having mean pore size of 0.45 micron. All the experiments were done in triplicate and demonstrated to be reproducible (error below 5 %); reported data representing the average values.

2.3 Spin Trapping Electron Spin Resonance (ESR) Measurements

The formation of paramagnetic species in solution during irradiation of the carbon suspensions was detected by a nitrone spin trapping agent (5,5-dimethylpyrroline-N-oxide, DMPO). This compound is capable of forming spin adducts with hydroxyl and superoxide radicals (see example in Scheme 1), creating more stable nitrone radicals that are easily

detected by ESR spectroscopy in aqueous solution [7]. About 0.5 g/L of the carbon samples were suspended in 5 ml of $HClO_4$ buffer (pH 3), and the appropriate volume of DMPO was added to the suspension to reach a final concentration of 18 mM. Samples were introduced in capillary quartz tubes and irradiated for 5, 10, 20 and 60 minutes (Philips TL K40W/05 lamp, with a broad emission peak centred at 365 nm). ESR spectra were immediately recorded from the solution (after filtering out the solids) at room temperature on a Bruker ESP 300E X band spectrometer with the following spectral parameters: receiver gain 105; modulation amplitude 0.52 G; modulation frequency 100 KHz, microwave frequency 9.69 GHz; microwave power 5.024 mW; conversion time 40.96 ms; center field 3450 G, sweep width 120 G. Simulations of the individual components of the ESR spectra were obtained using the Winsim 2002 software [10].

3. Results and discussion

A series of semiconductor-free carbon materials with varied structural, textural and chemical composition have been investigated. The choice of these carbons was made based on their ability to promote the photooxidation of phenol when exposed to UV light in the absence of other semiconductors, as revealed by photocatalytic tests reported in previous studies [4,5]. A summary of phenol photodegradation efficiency of herein reported materials is shown in Fig.1 for data interpretation. Briefly, high phenol conversions were obtained after UV irradiation of all these materials, along with a sharp reduction in the Total Organic Content (TOC) values in solution. These results indicated the ability of these carbon photocatalysts to promote the photooxidation of phenol in the absence of conventional semiconductor catalysts (i.e., titanium dioxide). To shed light on the origin of this anomalous behavior, and to link the photodegradation performance of the carbons with their physicochemical features, we have carried out a spin resonance (ESR) spectroscopy study.

Fig. 2 shows the ESR spectra of the DMPO adducts obtained after 20 minutes irradiation of the studied carbons. Data corresponding to the ESR spectrum obtained for commercial TiO_2 powders (Evonik) has also been included for comparison purposes. It should be highlighted that no ESR signals were observed when the measurements were performed in dark conditions (absence of UV light) for any of the catalysts, or when DMPO alone was irradiated. Additionally, the intensities of the ESR signals of all the samples gradually increased with time showing a maximum at 20 min, which confirmed the formation of DMPO adducts at short irradiation times.

The ESR spectra of the carbon samples showed a quartet peak profile with 1:2:2:1 intensity (circles) at g = 2.006 with aN = aβH = 14.8 G hyperfine splitting constants. This is consistent with the spectra reported in the literature for the DMPO-OH adducts [7,8] and confirms the formation of significant amounts of •OH radicals during the irradiation of the carbons, likely produced from photoinduced oxidation of water -the reaction medium during the illumination of the carbons suspensions-. Although increased concentrations of •OH radicals have been reported for carbon nanotubes/titania composites [11], our results demonstrate the formation of radicals upon UV irradiation of carbon materials in the absence of semiconductor additives like titanium oxide, zinc oxide, etc. Spin trap ESR experiments also show the formation of hydroxyl radical-like species in irradiated TiO_2 suspensions, in agreement with the literature [12]. It is interesting to point out that the DMPO-OH concentration levels measured for certain carbons were higher than those obtained from titania powders under the present experimental conditions.

Although UV irradiation of the aqueous dispersions of carbon materials resulted in ESR spectra characteristic of DMPO-OH adducts, this signal cannot be exclusively assigned to hydroxyl radicals but could also suggest the occurrence of superoxide radical. In fact it is well

known that the superoxide anion is unstable in water medium being converted to •OH radical and eventually contributing to the DMPO-OH adduct signal [13,14].

Moreover, although DMPO-OH is the dominant adduct, simulation of the experimental spectra (Fig. 3) allowed the identification of additional adducts, less intense, for some of the samples as indicated in Fig. 2. Based on the simulated hyperfine splitting constants (Table 3) these were identified as HDMPO-OH (aN=14.6 G, aγH=1.1 G) [8], a carbon centered radical with DMPO-R (aN=15.4 G, aβH=22.9 G) and the DMPO-OOH adduct (aN=14.7 G, aβH=10.5 G, aγH=1.1 G) originated upon reaction with superoxide radical anion [11].

Such complex patterns are a diagnostic indication of free hydroxyl radical formation in aqueous environments [11], and constitute a key issue on the understanding of the recently reported photochemical response of carbon materials under UV irradiation, through a radical-mediated pathway for most of herein studied carbons. Only for one of the studied carbons (samples AC4) no radical formation was detected upon irradiation of the carbon aqueous suspension. This is in agreement with the lack of photoactivity observed for this activated carbon in previous works [5] and demonstrates that formation of photoinduced radicals is not an intrinsic property of all carbon materials.

The complex ESR patterns overimposed to the 1:2:2:1 quartet were more evident in the non-porous carbons (Fig.2 bottom), although with much lower intensities and suggests a low efficient detection of radicals in nanoporous materials. This seems rather reasonable considering two facts; the first one is the tortuosity of porous networks, which would impose a restricted diffusion of the radicals trapped inside the pores through the bulk solution, and thus they would decompose before reacting to form the spin adducts that are detected in the bulk solution. On the other hand, DMPO-radical adducts might be retained in the porosity of the carbons, and thus the concentration detected in solution would be lower.

On the other hand, the low intensity of the additional adducts seems reasonable since it is well known that DMPO-OOH adducts have short half lifetimes in water and easily undergo disproportionation [15]. Additionally, the kinetics of the reactions between •OOH and DMPO are typically much slower than that reported for the formation of the DMPO–OH spin adduct [16,17].

Quantification of the relative abundance of the radical species formed was also possible from the ESR measurements. Due to the overall poor signal/noise ratio in certain samples, the quantitative analysis was performed over the intensity of the line showing the highest signal/noise ratio –second peak in the 1:2:2:1 quartet profile-, for an irradiation time fixed at 20 min. Comparative data is shown in Fig. 4.

As mentioned above, the comparison between porous and non-porous materials might not be straightforward if we consider that a fraction of the photogenerated radicals and/or DMPO spin adducts could be eventually trapped inside the porosity of the carbons and thus would not be detected. In such situation, the concentration of radical species would be higher than the actual value measured in the bulk solution; anyhow, comparison of the quantitative data renders interesting observations. For some of the studied carbons, the intensity of the second peak used for quantification was larger than that of a widely used TiO_2 (P25, Evonik), indicating a higher concentration of radical species detected despite the porosity of the carbons.

Although a univocal correlation between the characteristics of the studied carbons and the formation of radicals cannot yet be identified, some trends may be postulated based on their chemical characteristics. First of all, the low ash content of some carbons (AC3, AC6, CS and CSH800) showing large ESR signals confirms the formation of radicals due to carbon-light interactions rather than to semiconducting elements present on the inorganic matter of the studied carbons. This is particularly remarkable on the samples prepared by hydrothermal

carbonization of glucose (CS and CSH800), both characterized by a negligible ash content (Table 1). Additionally, comparison of AC5 with its corresponding de-ashed counterpart (carbon AC6) demonstrates even though the ESR signal of the pristine carbon is reduced after the complete removal of the inorganic matter, radical species are formed on irradiation of the ash-free carbon matrix [18]. Moreover, the intensity of the second peak in the ESR spectra in the de-ashed carbon is ca. 1.5 times higher that the value measured for titanium dioxide under similar conditions, and within the highest values retrieved for the series of studied carbons. Concerning the effect of the surface chemistry, as a general rule the presence of O-containing functionalities on the carbon matrix seems to have a negative impact on the detection of radicals as inferred by the low ESR intensities detected for carbons AC2 and CS, compared to those of ca. AC3 which displayed much lower oxygen content (Table 2) and lower concentration of surface functionalities [5]. However, this dependence is not straightforward as the thermal annealing of CS at 800 ºC under inert atmosphere to remove all the surface functionalities (sample CHS800) resulted in a slight decrease in the amount of radical species detected (Fig. 4), as opposed to expectations based on the above-mentioned general rule considering the oxygen content of these carbons (Table 2). Also, the intensity of the second peak in the ESR spectra was almost three times higher for sample CS than AC2, despite the much higher oxygen content of the former. This fact points out that the nature of the surface functionalities might also be important for the detection of the radical species. Differences in the surface chemistry of these two materials were pointed out by quantification of the thermodesorbed species by TPD-MS (Fig. 5) and measurement of the surface acidity. Data showed a higher acidic of AC2 (i.e., pH_{PZC} ~2.2 and 3.5 for AC2 and CS, respectively), which is attributed to larger amounts of carboxylic acids (as CO_2-evolving groups below 400 ºC), whereas lactones, phenols and carbonyl/quinone-type groups (decomposing as CO and CO_2 above 600 ºC) are predominant for CS. In fact, there seems to be a correlation with the

acidic/basic character of the carbons: the more acidic the PZC of the carbons, the lower the signal of the ESR spectra (Table 2); again sample CSH800 breaks this trend indicating that the issue is more complex and cannot be attributed to one single parameter.

Other than oxygen, the role of other heteroatoms can also be speculated; the high ESR signal of carbons AC5 and AC3 could also be related to traces of sulfur and/or nitrogen surface groups also detected in these materials; indeed, the effect of sulfur on the visible light photoactivity of S-doped carbons has been recently reported [19]. In the case of AC5, there is also a significant formation of DMPO-OOH adduct, suggesting a higher reaction with molecular oxygen.

It should be noted that despite the low concentration of radical species, some of these carbons showing a rich chemistry (carbon AC2) displayed among the highest photoactivity towards phenol and photooxidation (Fig. 1), higher than other carbons with larger ESR signals. Hence, low ESR signals should not be considered as an indication of low photoactivity, since this technique only provides information about the formation of radicals under irradiation of the studied materials. Indeed, a similar behavior has been reported for some titanium oxides powders (no ESR signal but non negligible phenol conversion) and has been attributed to different active sites in the semiconductor that can favor either a radical-like mechanism or direct hole transfer [20]. In the case of the some of the carbons studied, the low ESR signals coupled with high photodegradation phenol conversions suggests a direct photooxidation mechanism not involving radicals.

Moreover, radical species were detected when irradiating carbons with both graphitic (GR1) and turbostratic (disorganized) structures; unfortunately, no clear tendency could be withdrawn so far concerning the effect of the structural order of carbon materials, suggesting that a more systematic study is needed to isolate all these effects. Further research is currently ongoing to clarify this issue.

The basis of the carbon-light interactions could be linked to the excitation of different electronic states (π–electron density, defect sites or vacancies) in the graphene layers of the carbons. Direct π–π* transitions due to the absorption of photons by the carbon matrix have been proposed for graphite and glassy carbon [21], whereas electronic transitions involving carbene-like structures at free zig-zag sites have been postulated to explain the photoluminescence of carbon nanostructures (i.e., carbon nanotubes and quantum dots) [21,22]. The photogeneration of electronic transitions due to UV excitation of the π-electron density, defects and vacancies seems most plausible, given that activated carbons (most of herein studied materials) can be considered as assemblies of defective graphene layers in a turbostratic structure. However, discriminating whether if UV light absorption leads to π–π* transitions or other electronic transitions involving, for instance, carbene-like structures at free zig-zag sites [23] still remains rather challenging since it requires a deep knowledge on the electronic structure of carbon materials. Anyhow, ESR measurements provided experimental evidence on the fate of the photoexcited electronic states of carbon materials which, in the presence of water and/or dissolved oxygen, stabilize through the generation of radicals. These radicals account for the reported photoactivity of herein studied carbons towards the photooxidation of aromatic compounds (Fig. 1).

4. CONCLUSIONS

Spin trapping ESR experiments have demonstrated that radical species (mainly hydroxyl and/or superoxide radicals) are formed when aqueous suspensions of carbon materials are exposed to UV light. Preliminary data has disclosed their capacity to generate a similar or even higher quantity of radicals than titania powders. These reactive species can effectively react with aromatic compounds and thus account for the reported photooxidation of pollutants

in certain carbons. More importantly, this ability has been detected for amorphous carbons with a disorganized structure (i.e. turbostratic), and did not seem to be exclusively related to carbon nanostructures with a graphitic structure.

These findings constitute the first step towards the understanding of the photoinduced reactions occurring at semiconductor free carbon materials through the photogeneration radicals in aqueous environments. Although more efforts are needed to further comprehend the light-carbon interactions, we believe this provides new perspectives on the understanding of the role of carbon materials in photocatalysis, as it demonstrates that the photooxidation of organic pollutants in the presence of carbons should be proposed as Advanced Oxidation Process.

ACKNOWLEDGMENTS

The authors thank the financial support of MICINN (grants CMT2008/01956 and CTM2011/23378) and FICYT (PC10-02). LFV thanks CSIC for her JAE-pre contract.

REFERENCES

[1] N. Serpone, E. Pelizzetti, Photocatalysis: fundamental and applications, Wiley Interscience, New York, 1989.

[2] M.A. Henderson, Surf. Sci. Reports 66 (2011) 185-297.

[3] R. Leary, A. Westwood, Carbon 49 (2011) 741-772.

[4] L.F. Velasco, J.B. Parra, C.O. Ania Appl. Surf. Sci. 256 (2010) 5254-5258.

[5] L.F. Velasco, I.M. Fonseca, J.B. Parra, J.C. Lima, C.O. Ania, Carbon 50 (2012) 249-258.

[6] J. Matos, J.M. Chovelon, T. Cordero, C. Ferronato, The Open Environ. Eng. J. 2 (2009) 21-29.

[7] E. Finkelstein, G.M. Rosen, E. Rauckman, J. Arch. Biochem. Biophys. 200 (1980) 1-16.

[8] K. Makino, A. Hagi A, H. Ide, A. Murakami, M. Nishi, Can. J Chem. 70 (1992) 2818-2827.

[9] J.A. Korver, Chemical Weekblad 46 (1950) 301-302.

[10] D.R. Duling, J. Magn. Res. Series B 104 (1994) 105-110.

[11] Y. Yu, J.C. Yu, C.-Y. Chan, Y.-K. Che, J.-C. Zhao, L. Ding, W.-K. Ge, P.-K. Wong, App. Catal. B. Environ. 61 (2005) 1–11.

[12] M.A. Grela, M.E.J. Coronel, A.J. Colussi, J. Phys. Chem. 100 (1996) 16940-16946.

[13] E. Finkelstein E, G.M. Rosen, E.J. Rauckman, J. Paxton, J. Mol Pharmacol. 16 (1979) 676–685.

[14] B. Gray, A.J. Carmichael, Biochem. J. 281 (1992) 795-802.

[15] G.R. Buettner, Free Rad. Res Comm. 19 (1993) 79-87.

[16] C.C. Chen, W.H. Ma, J.C. Zhao, J. Phys. Chem. B 106 (2002) 318-24.

[17] A. Bosnjakovic, S. Schlick, J. Phys. Chem. B 110 (2006) 10720-28.

[18] L.F. Velasco, V. Maurino, E. Laurenti, I.M. Fonseca, J.C. Lima, C.O. Ania, Apll. Catal. A General, 2012 (accepted)

[19] T.J. Bandosz, J. Matos, M. Seredych, M.S.Z. Islam, R. Alfano, Appl. Catal. A: General, 2012 (doi: 10.1016/j.apcata.2012.08.020)

[20] C. Minero, A. Bedini, V. Maurino, Appl. Catal. B: Environ. 128 (2012) 135-143.

[21] A.D. Modestov, J. Gun, O. Lev, Surf. Sci. 417 (1998) 311-22.

[22] Q. Bao, J. Zhang, C. Pan, J. Li, C. Li, J. Zang, D.Y. Tang, J. Phys. Chem. C 111 (2007) 10347-52.

[23] D. Pan, J. Zhang, Z. Li Z, M. Wu, Adv. Mater. 22 (2010) 734-38.

Figures Captions

Scheme 1. Formation of spin-adduct DMPO-OH (DMPO = 5,5-dimethyl pyrroline-N-oxide).

Figure 1. Comparative phenol photooxidation efficiency of the investigated semiconductor-free photocatalysts in terms of phenol disappearance (black) and reduction in the Total Organic Carbon values (grey) retrieved in solution after 6 hours of irradiation. Initial TOC value was 76.5 mg C l^{-1} in all cases.

Figure 2. Comparative of the ESR signals obtained upon 20 minutes irradiation of aqueous suspensions of selected carbon materials and titania powders. Assignments to DMPO-OH (circles), HDMPO-OH (diamonds) and DMPO-OR (squares) adducts are indicated.

Figure 3. Experimental (top, black) and simulated (down, red) ESR spectra of the studied carbons and commercial titania powders (P25 from Evonik).

Figure 4. Quantification of the radical species detected from the ESR signals corresponding to DMPO-OH adducts.

Figure 5. CO and CO_2 profiles of the carbons AC2 (triangles), CS (squares) and CSH800 (circles).

Tables Captions

Table 1. Main textural characteristics of the selected carbon materials and the titania powders used as reference photocatalyst.

Table 2. Chemical composition (wt.% on dry basis) of the selected samples and surface acidity estimated by the Point of Zero Charge (pH_{PZC}).

Table 3. ESR parameters of the radical species formed upon UV irradiation of the investigated carbon materials and commercially available TiO_2 (Evonik).

Table 1. Main textural characteristics of the selected carbon materials and the titania powders used as reference photocatalyst.

	Remarks	S_{BET} ($m^2\ g^{-1}$)	V_{TOTAL} [A] ($cm^3\ g^{-1}$)	$V_{MICROPORES}$ [B] ($cm^3\ g^{-1}$)	$V_{MESOPORES}$ [B] ($cm^3\ g^{-1}$)
TiO_2 (P25, Evonik)	Commercial titania powders	57	0.18	0.006	0.08
AC1	Activated carbon, steam activation coal, labeled as Q in ref. 12	1033	0.52	0.32	0.09
AC2	Activated carbon, chemical activation lignocellulosic residue, labeled as CV in ref. 12	1280	1.06	0.31	0.52
AC3	Activated carbon, steam activation coal, labeled as FY5 in ref. 12	799	0.35	0.26	0.03
AC4	Activated carbon, steam activation plastic residue, labeled as PC in ref. 12	1357	0.60	0.45	0.04
AC5	Activated carbon, steam activation, labeled as BKK in ref. 12	961	0.57	0.29	0.06
AC6	De-ashed AC3 by acid digestion in HF/HCl at room temperature	752	0.32	0.24	0.01
GR1	AC1 graphitized at 2400ºC	33	0.08	0.00	0.01
CS	Carbon spheres, hydrothermal carbonization polysaccharides	10	0.02	0.01	0.01
CSH800	Sample CS after thermal annealing at 800ºC under N_2 atmosphere	569	0.33	0.18	0.01

[A] evaluated at p/po ~ 0.99

[B] evaluated by NLDFT method

.

Table 2. Chemical Composition (wt.% on dry basis) of the Selected Samples and surface acidity estimated by the Point of Zero Charge (pH_{PZC}).

	C (wt. %)	O (wt.%)	H (wt. %)	S (wt.%)	N (wt.%)	Ash (wt.%)	pH_{PZC}
AC1	85.5	1.9	0.4	0.1	0.5	11.4	8.9
AC2	86.2	9.7	2.8	0.1	0.3	0.9	2.2
AC3	94.1	2.7	0.8	0.1	0.3	2.0	9.0
AC4	99.2	0.6	0.3	n.d.	n.d.	n.d.	10.9
AC5	90.5	4.5	0.3	0.2	0.8	3.8	8.5
AC6	96.4	2.8	0.8	n.d.	n.d.	n.d.	3.3
GR1	96.4	n.d.	0.2	< 0.1	n.d.	3.3	6.5
CS	70.4	24.8	4.6	n.d.	n.d.	n.d.	3.5
CSH800	90.3	8.8	0.9	n.d.	n.d.	n.d.	6.8

n.d. not detected

Table 3

Table 3. ESR parameters of the radical species formed upon UV irradiation of the investigated carbon materials and commercially available TiO_2 (Evonik).

		AC1	AC2	AC3	AC4	AC5	AC6
DMPO-OH	aN	14.97	14.98	15.02	--	14.99	14.96
	aH(β)	14.68	14.68	14.59	--	14.59	14.66
	%	100	100	80.9	--	58.2	43.8
HDMPO-OH	aN	--	--	14.55	--	14.37	14.63
	aH(γ)	--	--	1.05	--	0.87	1.10
	%	--	--	19.1	--	4.3	56.2
DMPO-OOH	aN	--	--	--	--	14.73	--
	aH(β)	--	--	--	--	10.42	--
	aH(γ)	--	--	--	--	1.06	--
	%	--	--	--	--	37.5	--
		TiO_2	GR1	CS	CSH800		
DMPO-OH	aN	14.95	15.07	15.03	15.02		
	aH(β)	14.67	14.57	14.56	14.51		
	%	80.3	60.9	36.5	68.3		
HDMPO-OH	aN	14.86	14.64	14.71	14.69		
	aH(γ)	1.01	1.19	0.93	1.09		
	%	19.7	16.9	22.6	31.7		
DMPO-R	aN	--	15.42	15.48	--		
	aH(β)	--	22.89	22.93	--		
	%	--	21.1	40.9	--		

Figure 1

Click here to download high resolution image

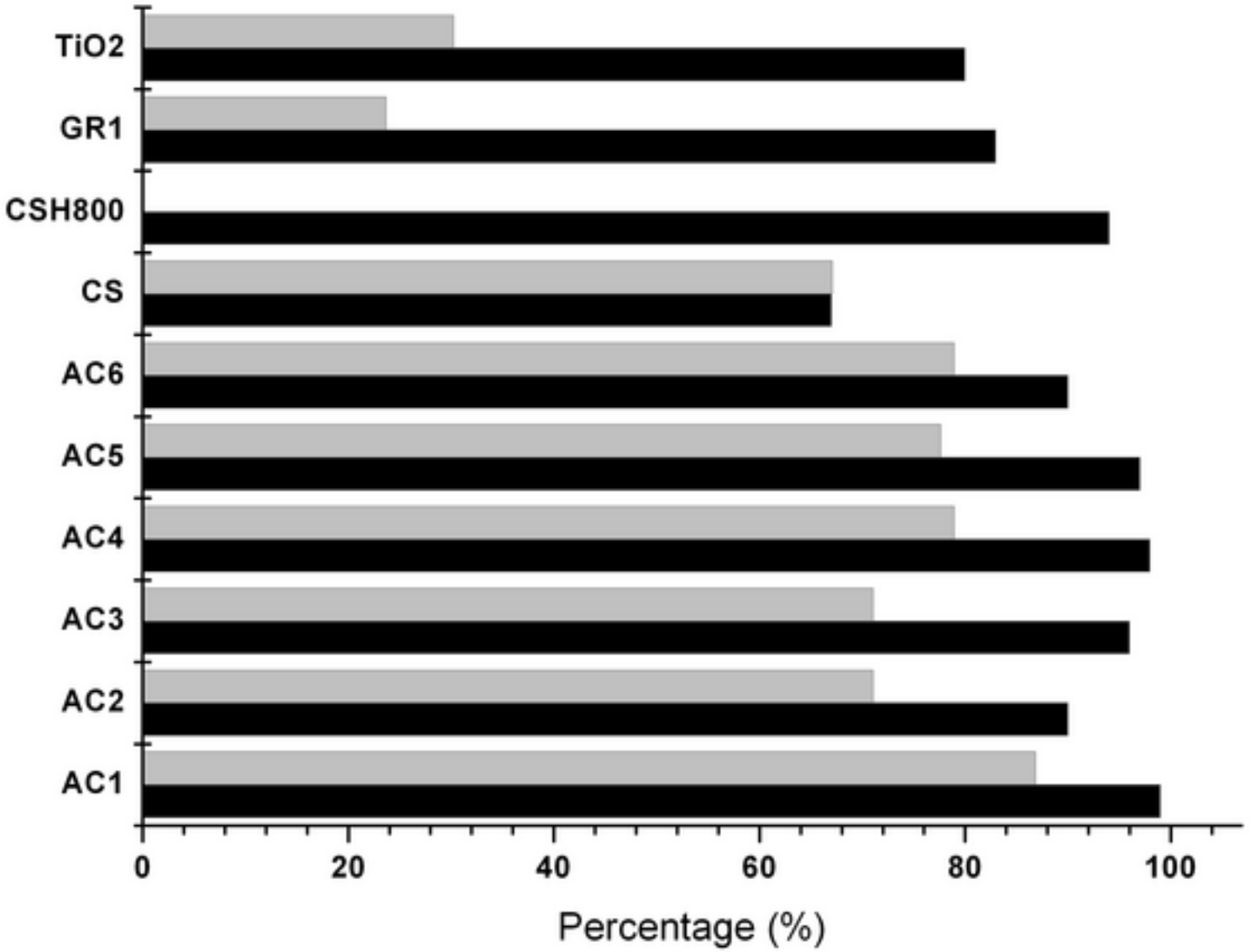

Figure 2

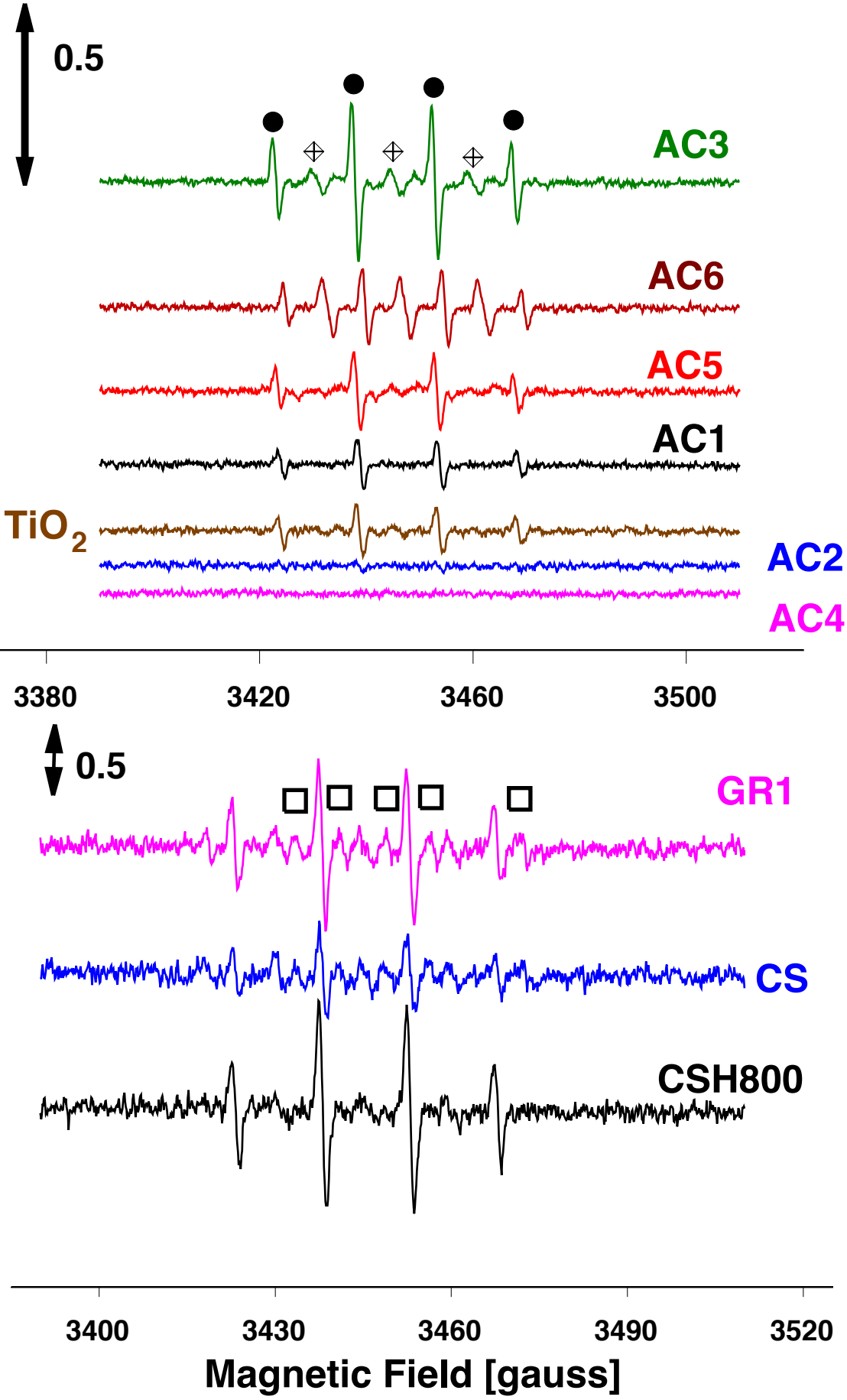
0.5
AC3
AC6
AC5
AC1
TiO2
AC2
AC4
3380
3420
3460
3500
0.5
GR1
CS
CSH800
3400
3430
3460
3490
3520
Magnetic Field [gauss]

Figure 3

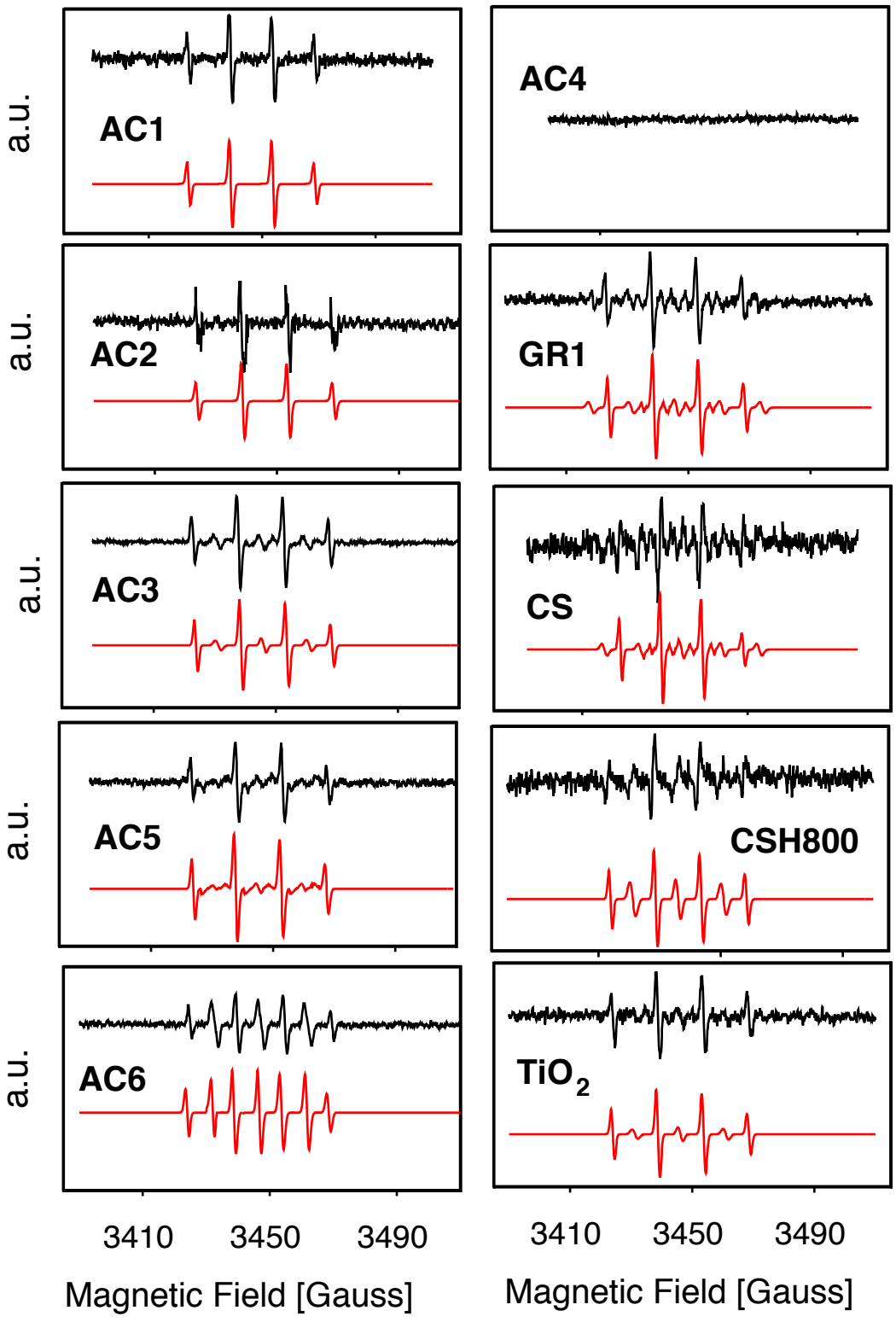
a.u.
AC1
AC4
AC2
GR1
AC3
CS
AC5
CSH800
AC6
TiO2
3410
3450
3490
Magnetic Field [Gauss]
3410
3450
3490
Magnetic Field [Gauss]

Figure 4

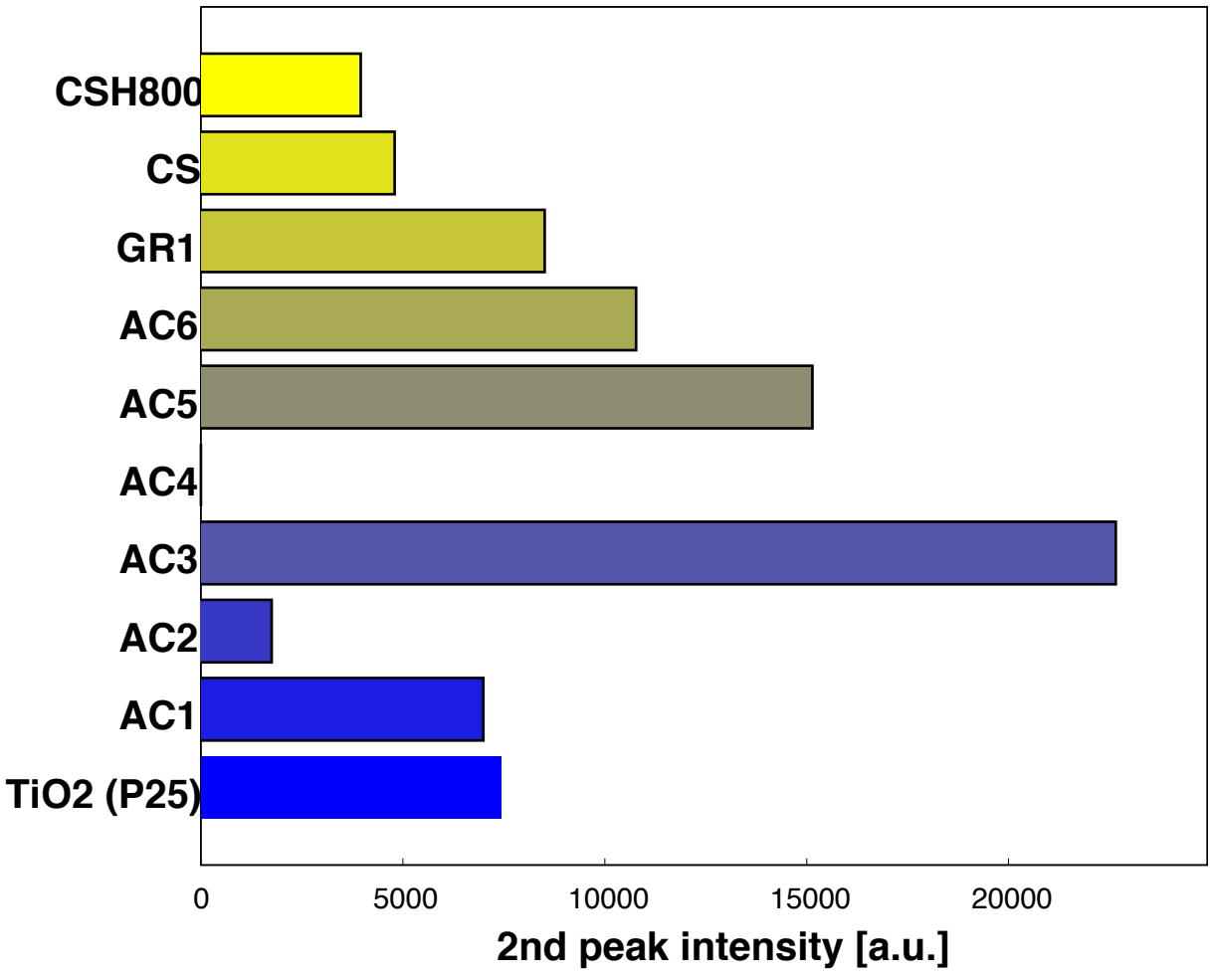
CSH800
CS
GR1
AC6
AC5
AC4
AC3
AC2
AC1
TiO2 (P25)
0
5000
10000
15000
20000
2nd peak intensity [a.u.]

Figure 5

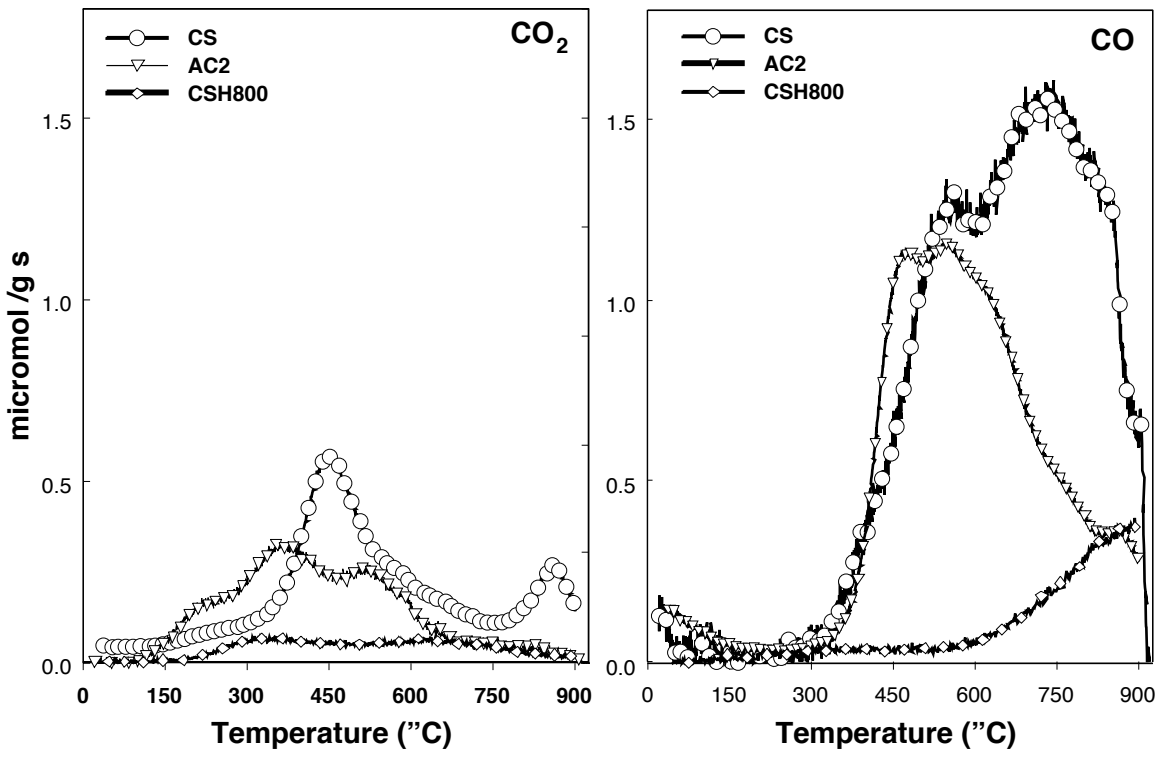
CS
AC2
CSH800
CO_2
micromol /g s
1.5
1.0
0.5
0.0
0
150
300
450
600
750
900
Temperature (”C)
CS
AC2
CSH800
CO
1.5
1.0
0.5
0.0
0
150
300
450
600
750
900
Temperature (”C)

Scheme 1

Click here to download high resolution image